ISSN 0031-918X, The Physics of Metals and Metallography, 2015, Vol. 116, No. 9, pp. 917–924. © Pleiades Publishing, Ltd., 2015.
Original Russian Text © V.M. Nadutov, D.L. Vashchuk, P.Yu. Volosevich, V.Z. Spuskanyuk, A.A. Davidenko, 2015, published in Fizika Metallov i Metallovedenie, 2015, Vol. 116, No. 9, pp. 966–973.

STRENGTH AND PLASTICITY

Structure Changes in Invar Fe–Ni and Fe–Ni–C Alloys under the Deformation by Upsetting

V. M. Nadutov[a], D. L. Vashchuk[a], P. Yu. Volosevich[a], V. Z. Spuskanyuk[b], and A. A. Davidenko[b]

[a] *Kurdyumov Institute of Metal Physics, National Academy of Sciences of Ukraine, bul. Akademika Vernadskogo 36, Kiev, 03680 Ukraine*

[b] *Galkin Donetsk Physicotechnical Institute, National Academy of Sciences of Ukraine, ul. Rozy Lyuksemburg 72, Donetsk, 83115 Ukraine*

e-mail: nadvl@imp.kiev.ua

Received May 15, 2014; in final form March 25, 2015

Abstract—Changes in the dimensional and microstructural characteristics of the samples of two invar fcc alloys, Fe–35.0% Ni–0.49% Mn and Fe–30.9% Ni–1.23% C, have been investigated by X-ray diffraction, metallographic, and electron-microscopic methods after upsetting with the logarithmic deformations $e = 0.5$ and 1.1. It has been shown that the regularities of changes in the macroscopic dimensions of the samples, as well as in the parameters of structural elements, which are presented by coefficients of the shape change after upsetting, are common for both alloys, although they have some distinctions. These distinctions are caused by the presence of a second phase in the carbon-containing alloy, which is concentrated predominantly along the boundaries of structural elements and affects the changes in the size and microstructural characteristics, as well as by a higher density and greater uniformity of the defect distribution.

Keywords: invar, structure, hardness, upsetting

DOI: 10.1134/S0031918X15090124

INTRODUCTION

One of the widely used industrial methods of fabricating metallic billets and articles is upsetting, theoretical foundations of which and specific features of plastic deformation upon such a treatment are rather well studied for alloys with fcc and bcc structures (copper, aluminum, iron [1–4]; steel [5]) both in a part of changes in the shape and dimensions of the samples and their microstructure.

The method is simple, but the sample is deformed nonuniformly over the volume [2] (Fig. 1). Due to the surface friction, zones I, in which the forming is minimum, arise in the contact regions. Zone II is subjected to maximum deformation and refinement of the structure. The degree of participation in the plastic deformation and, consequently, the structure of zone III, which is located along the side surface of the cylinder, depends, similarly to zones I and II, on the amount of plastic deformation.

The results of microhardness measurements over the height in the central part of the samples, which were performed, in particular with the imposition of ultrasonic vibrations during upsetting, confirm the nonuniformity of the deformation distribution [6–9]. The authors of [10] experimentally revealed a nonmonotonic variation of hardness and electrical resistivity of grade-20 steel under stepped upsetting, which also is caused by the deformation nonuniformity in various zones.

At the same time, considerably less attention has been paid to the investigation of the formation of the fine structure under similar types of treatment in the case of iron-based bcc and fcc alloys, including two-phase alloys. In particular, the structure and properties of invar Fe–Ni alloys after the deformation by upsetting have virtually not been studied, although this technology is widely used to fabricate articles from these alloys. The data concerning the interrelation between the changes in the shape of microstructure elements of invar alloys after upsetting and the geometrical sizes of metallic billets are also absent. In

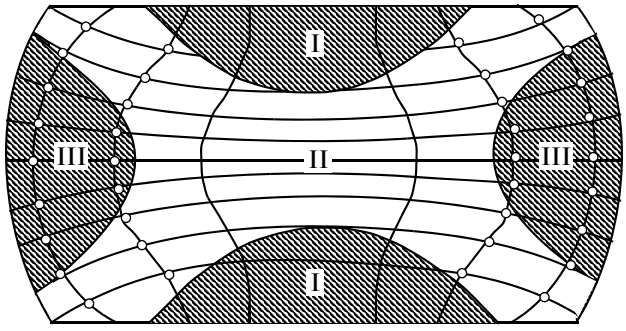

Fig. 1. Distribution of accumulated plastic deformation upon upsetting over the longitudinal section of a billet (schematic) [2].

Table 1. Chemical composition of the 1N31 alloy

Alloy	Content of alloying elements, wt %				
	Ni	C	Cr	Cu	Fe
1N31	30.9	1.23	<0.003	<0.03	For balance

addition, it has not been studied how carbon affects the formation of the fine structure in fcc Fe–Ni alloys during upsetting.

Therefore, this study was aimed at the establishment of regularities of the structure formation in Fe–Ni and Fe–Ni–C invar alloys after upsetting deformation and at the investigation of correlation between the forming of its elements and the geometric parameters of ingots, as well as the metal hardness over the height of ingots after upsetting to logarithmic deformation $e = 0.5$ and 1.1.

EXPERIMENTAL

This study was performed using the industrial invar alloy N36 (Russian State Standard GOST 10994-74) of composition Fe–35.0Ni–0.49Mn (wt %), and a laboratory carbon-containing alloy 1N31, the composition of which is presented in Table 1.

The samples for the tests were cylinders with diameters of 12.5 and 21 mm and a height of 25 and 30 mm for the alloys N36 and 1N31, respectively. They were first homogenized at 1373 K in a silicate slag with holding for 30 min, then quenched in room-temperature water. The slag was used to prevent sample oxidation and to minimize carbon loss.

After heat treatment (initial state), the billets were deformed by upsetting under a force of 1 MN at the velocity of the press slider $V_s = 2$ mm/s. Deformation under upsetting was determined from the expression

$$e = \ln\frac{h_0}{h}, \quad (1)$$

where h_0 and h are the sample heights before and after the upsetting, respectively.

The structure and the properties of both alloys after the upsetting treatment were investigated by X-ray diffraction, metallography, and electron microscopy, as well as by the hardness method.

The metallographic investigations were performed using a NEOPHOT-32 optical microscope in transverse (parallel to the plane of the contact surface) and longitudinal (along the height) sections of the middle part of the sample using polished sections prepared by the mechanical and electrolytic methods of polishing (etching) in the electrolyte of the following composition: 75 g chromium anhydride, 133 mL glacial acetic acid, and 20 mL water at a voltage of 90 V and a current of 0.5–1.5 A. This electrolyte was also used when preparing thin foils for investigations by transmission electron microscopy (using a JEM-2000 FX device), the samples for which were cut from the central part of the longitudinal and transverse sections of ingots.

The dislocation density in the deformed states of the alloys was determined by the method of comparison with the generally accepted dislocation density in martensite (10^{11}–10^{12} cm^{-2}).

The X-ray diffraction analysis was performed using a DRON-3M diffractometer in Co $K\alpha$ radiation in the sample sections perpendicular to the upsetting direction.

The Vickers hardness under a load of 5 kg was determined along the sample height in the plane of the longitudinal section with a step of no more than two imprint diagonals. The measurement error was ± 10 HV_5.

The estimations of the size ($\langle d \rangle$) distribution of structure elements (grains) as well as of the relative changes in the diameters of the billets k_k and k_m, of the coefficients of grain elongation k_1 and k_1', and of the coefficient of variation of the average grain size k_{av} after the upsetting deformation were performed using the Image Pro 3.0 software (Table 2).

The relative changes in the diameters of billets were determined from the relationships

$$k_k = \frac{D_0}{D} \text{ and } k_m = \frac{D_0}{D_1}, \quad (2)$$

where D_0 is the diameter of the ingot cross-section in the initial state, before upsetting; and D and D_1 are the diameters of the sections of the near-surface and middle parts of the samples deformed by upsetting, respectively. The elongation coefficients of grains k_1 and k_1' in the longitudinal section in the near-surface

Table 2. Macroscopic and microscopic characteristics of forming of the billets of invar alloys and of their structure after the deformation by upsetting

Alloy	e	D_0, mm	D, mm	D_1, mm	h_0, mm	h, mm	k_k/k_m	k_c	k_1/k_1'
N36	1.1	21	34.8	37.9	30	9.8	0.60/0.55	0.77	0.29/0.16
1N31	0.5	21	24.8	26.8	25.0	15	0.84/0.78	0.91	0.39/0.37
1N31	1.1	12.5	17.2	20.0	25.0	8	0.72/0.63	0.78	0.29/0.27

and central parts of the samples were evaluated from the relationship

$$k_1, k_1' = \frac{\langle d_{\min} \rangle}{\langle d_{\max} \rangle}, \quad (3)$$

where $\langle d_{\min} \rangle$ and $\langle d_{\max} \rangle$ are the average minimum and maximum grain sizes. The quantity

$$k_{av} = \frac{\langle d \rangle_{init}}{\langle d \rangle_{def}} \quad (4)$$

is determined as the ratio of the average grain sizes on the surface perpendicular to the upsetting direction in the initial and deformed states.

RESULTS AND DISCUSSION

The analysis of the above results indicates that the changes in the macroscopic parameters of the samples expressed as the ratio of coefficients $k_k/k_m = 0.60/0.55$ for the N36 alloy correlate with the changes in the microscopic coefficients $k_1/k_1' = 0.29/0.16$, which indicates the formation of a texture, the degree of manifestation of which increases upon approaching the central part of the samples. A similar effect is also observed in the case of the 1N31 alloy (Table 2).

An analysis of the histograms of the size distribution of structure elements (grains), which were found from the results of metallographic investigations of the N36 alloy performed on the surface and middle parts of the sample deformed to $e = 1.1$ in the transverse and longitudinal sections, are presented in Fig. 2. They indicate that, after the above-mentioned deformation, an increase in the average grain size relative to the initial state by 30% (from 50 to 65 μm (Figs. 2e and 2f, respectively) is observed on the external (contact) surface of the sample section transverse to the upsetting direction (zone I, Fig. 1), with the conservation of the grain shape and without any signs of a preferential direction in the change in sizes.

A similar regularity is also observed in the middle part of the sample (Fig. 1, zone II): the average maximum grain size increases approximately twofold (from 52 to 110 μm) (Figs. 2e, 2h). In this case, the coefficient of the increase in the diameters of the samples (k_k/k_m) for both alloys varies proportionally to the degree of deformation (Table 2). At the same time, the investigations of the structure in longitudinal sections indicate an elongation of structure elements along the axis perpendicular to the sample height, which is increased on moving from the loading surface to the sample middle (Table 2, $k_1/k_1' = 0.29/0.16$ for the N36 alloy; the changes for the 1N31 alloy are similar). The character of changes in the elongation along the vertical axis has a parabolic dependence with a maximum in the middle part of the sample (Fig. 1).

The size distributions of structure elements (grains), which were determined from metallographic investigations of the 1N31 alloy after the deformations to $e = 0.5$ (Fig. 3) and 1.1 (Fig. 4) in the transverse and longitudinal sections in the surface and middle parts of the samples are presented in the histograms.

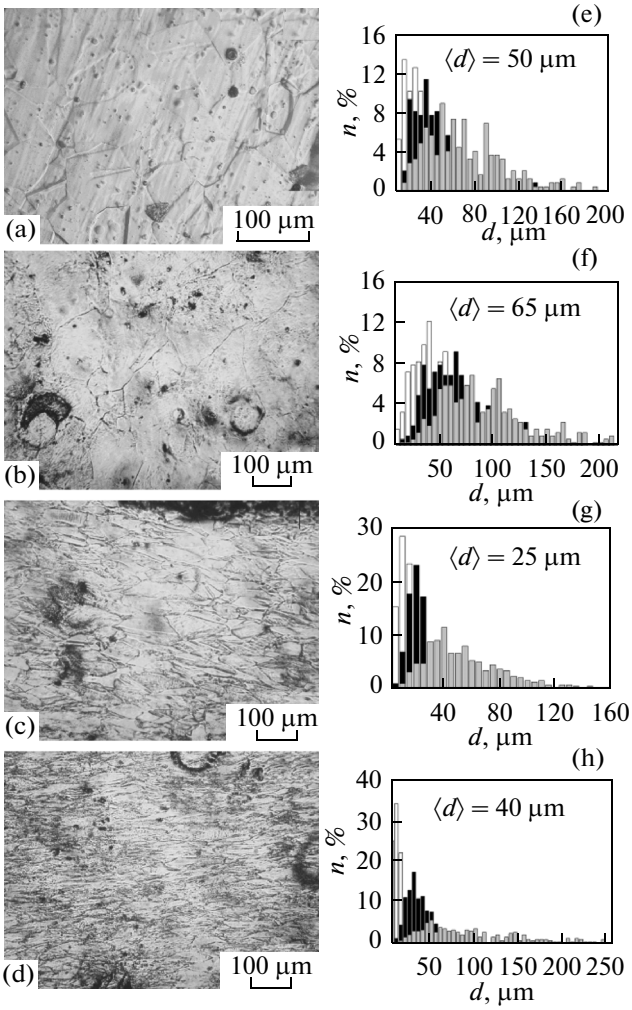

Fig. 2. Structures of the samples of the N36 alloy in the initial state (a) and after the upsetting to $e = 1.1$ in the transverse section (middle part) (b) and in longitudinal sections (c) in the near-surface part and (d) in the middle part of the sample, with corresponding histograms (e, f, g, h) of grain-size distributions by (○) minimum, (●) medium, and (●) maximum sizes.

They indicate that, on the external (contact) surface of the transverse sample section, an increase is observed in the average grain diameter relative to the initial state by 9.6% (Figs. 3e, 3f) and 28% (Figs. 3e, 4c), respectively, with the conservation of their shape. The variation of the average maximum grain size depending on the degree of deformation has an inverse character. In the longitudinal section of the sample of the 1N31 alloy, after $e = 0.5$, it decreases by 5% (Figs. 3d, 3g) and 11% (Figs. 3e, 3h), respectively, when moving from the surface to the middle part.

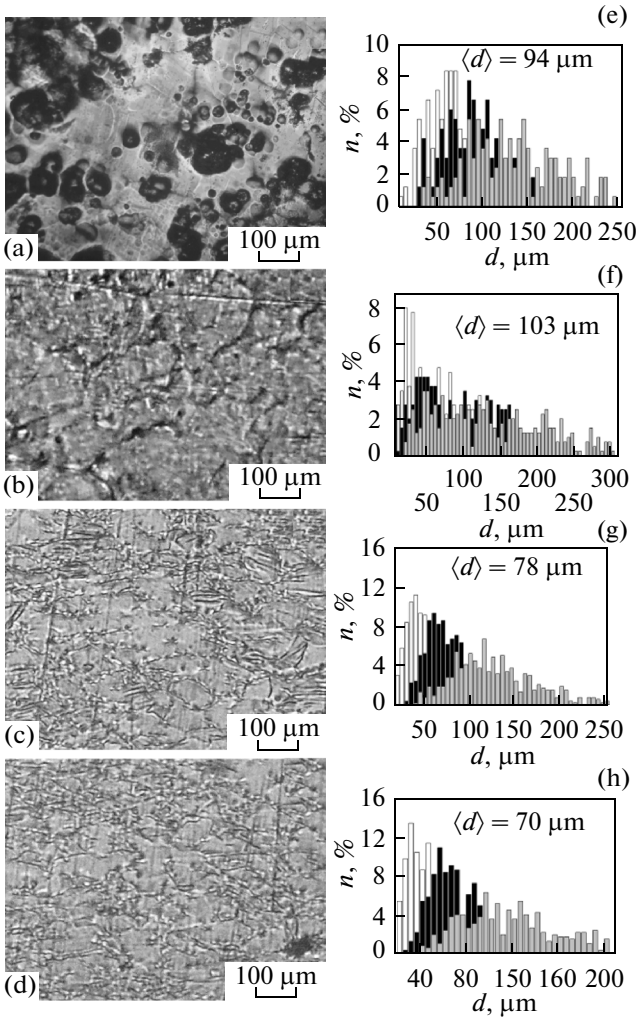

Fig. 3. Structure of the samples of the 1N31 alloy in the initial state (a) and after the upsetting deformation to e = 0.5 in the transverse section (middle part) (b) and in longitudinal sections (c) in the near-surface part and (d) in the middle part of the sample, with (e, f, g, h) corresponding histograms of grain size distributions by (○) minimum, (●) medium, and (◍) maximum sizes.

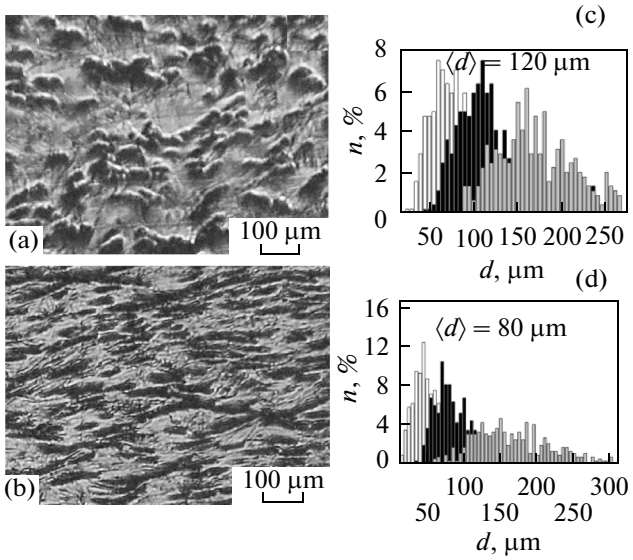

Fig. 4. Structures of the samples of the 1N31 alloy after the upsetting deformation to e = 1.1 in (a) transverse and (b) longitudinal sections of the near-surface part with (c, d) corresponding histograms of grain-size distributions by (○) minimum, (●) medium, and (◍) maximum sizes.

In this case, the relative change in the sizes of the deformed billets for the N36 and 1N31 alloys is proportional to the degree of deformation (Table 2; for example, h for the N36 alloy decreases from 30 to 9.8 mm with an increase in the diameter from 21 to 37.9 mm). At the same time, the structural investigations in the longitudinal sections indicate substantial changes, which are observed upon moving from the surface of the application of the force during upsetting to the middle of the samples (Figs. 2c, 2d, 3c, 3d). This is accompanied by a more or less uniform increase in the coefficients of elongation of the structure elements k_1 and k_1' from 0.29 to 0.16 for the N36 alloy.

The character of this variation is parabolic with a maximum in its middle part. Our results of metallographic investigations of the structures of both alloys evidence that, as compared to the N36 alloy, the 1N31 alloy (Figs. 3, 4) in the initial state has a grain structure in which the boundaries are decorated by globular and elongated graphite precipitates that are characteristic of the Fe–Ni–C austenitic alloys [11]. This circumstance apparently affects the general regularities of the formation of structures over the section of the samples, which manifest themselves in changes in the corresponding coefficients. A more considerable elongation of the structure elements is observed in the N36 alloy (k_1/k_1' = 0.29/0.16) compared with 1N31, where k_1 and k_1' are equal to 0.29 and 0.27, respectively, with the total decrease in the ratio of the coefficient of the variations in the macroscopic parameters of the samples k_k/k_m of the latter from 0.84/0.78 to 0.72/0.63 for e = 0.5 and 1.1, respectively (Table 2).

In addition to the above-mentioned features, rough traces of sliding arranged at angles of 35°–40° to the contact plane are observed upon the metallographic investigation of the longitudinal sections of both alloys in the near-contact layers.

The analysis of the results of the X-ray diffraction investigations (Fig. 5) indicates that the intensities of lines 200 and 311 for the N36 alloy decrease in the transverse section after upsetting to e = 1.1. This is the sign of the formation of a preferential crystallographic orientation of structure elements in the material.

Similar investigations performed for the 1N31 alloy indicate a considerable increase in the intensities of lines 111, 200, and 222 with an insignificant effect for the 311 line upon recording from the transverse section of the sample, whereas in the case of the longitu-

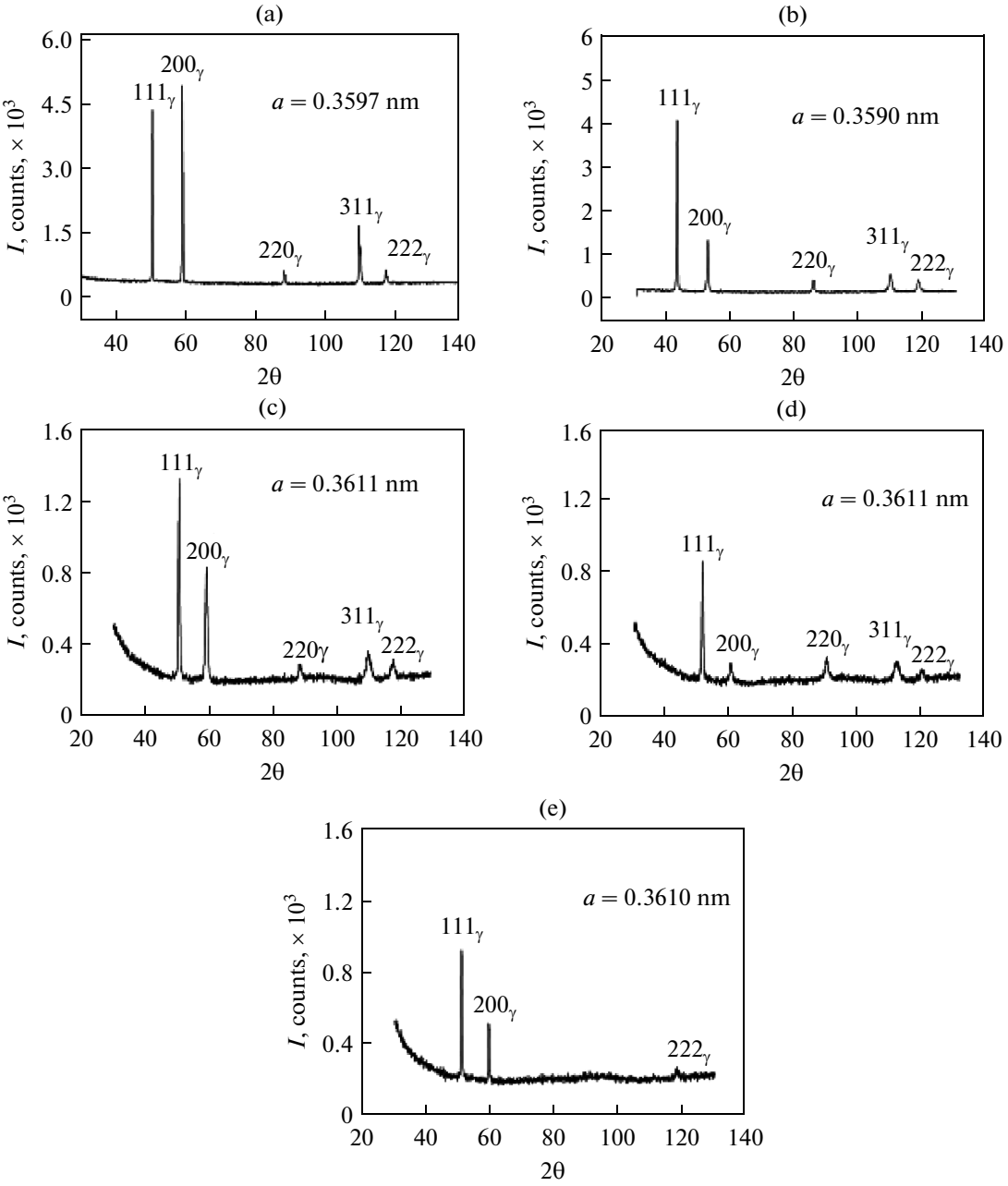

Fig. 5. X-ray diffraction patterns of the samples of alloys (a, b) N36 and (c–e) 1N31 in the initial state (a, c) and after the upsetting deformation to $e = 1.1$ in the transverse ((b) contact surface and (d) middle part of the sample and in the longitudinal sections (e).

dinal section, the lines 220 and 311 vanish at all. This indicates the formation of a sharper texture.

The analysis of the structure of the alloys studied in both sections of the central part of the samples by transmission electron microscopy of thin foils (Figs. 6, 7) shows that, in the N36 alloy, in the transverse section, the structure consists of almost uniaxial cells with sizes of 0.2–1.0 μm. The magnitude of the azimuthal smearing of reflections depends on the initial grain orientation, which varies in the limits of 5°–15°, which follows from an analysis of electron-diffraction patterns and dark-field images (Figs. 6b, 6c). The typical structure of the longitudinal section of the N36 sample is characterized by clearer boundaries of cells elongated predominantly in the direction normal to the upsetting direction. The sizes of structure elements lie in the limits of 0.5–3.5 μm with an elongation coefficient equal to 0.2 (Fig. 6d). The azimuthal misorientation of structure elements in the longitudinal section also depends on the orientation of the initial grains and lies in the limits of –2.5°...12°. The minimum grain size of structure elements of the longitudinal sec-

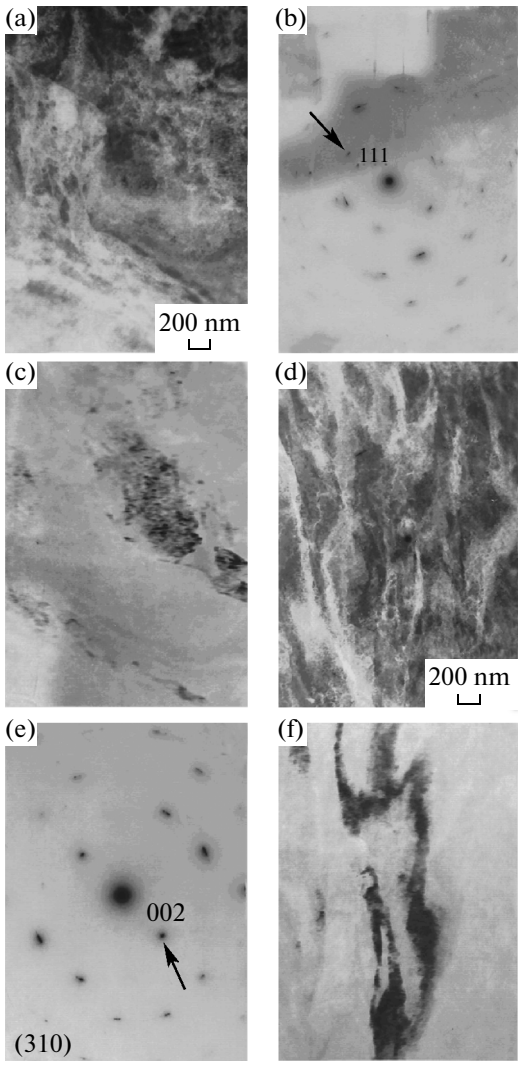

Fig. 6. (a, d) Typical microstructures of the N36 alloy in transverse and longitudinal sections of a sample after upsetting to $e = 1.1$; (b, e) electron-diffraction patterns from the regions shown in (b) and (e); and (c, f) dark-field images obtained in reflections indicated in (b, e), respectively.

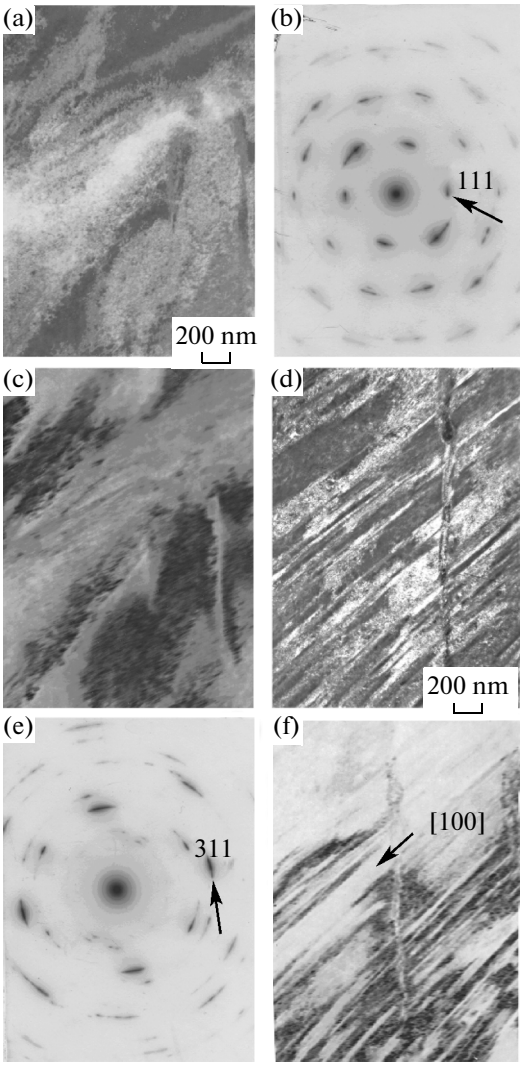

Fig. 7. (a, d) Typical microstructures of the 1N31 alloy in transverse and longitudinal sections of a sample after upsetting to $e = 1.1$; (b, e) electron-diffraction patterns taken from the regions shown in (b) and (d); and (c, f) dark-field images obtained in reflections indicated in (b, e), respectively.

tion is in the limits of 0.5–1.0 μm. The dislocation density inside the structure elements of both sections is on the a level of 10^{11} cm^{-2}. In the transverse section, the dislocations mainly form pileups and tangles (Fig. 6a), whereas in the longitudinal section, they are located mainly along the boundaries of the structure elements (Fig. 6d).

Compared with the N36 alloy, the structure of the 1N31 alloy in the central part of the samples and after upsetting is presented by elements, the boundaries of which in both sections are decorated by precipitates of the second phase (Fig. 4). In this case, their distribution correlates with the variations in the grain parameters, which, in the transverse section, increase in the direction from the surface to the sample center from 94 μm (initial state) to 100 and 120 μm depending on the degree of deformation ($e = 0.5$ and 1.1, respectively) with the practical absence of changes in shape (Fig. 3). At the same time, in the longitudinal sections there is observed a considerable elongation of structure elements, which is increased along the direction toward the sample center. This process is accompanied by corresponding changes in the arrangement of the second-phase inclusions, which decorate the boundaries of the initial grains.

The azimuthal misorientation of structure elements in the longitudinal sections depends on the grain orientation in the initial state and lies in the limits of 2.5°–12° (Fig. 7). The minimum size of the elongated elements lies in the limits of 0.03–0.4 μm,

with the maximum size reaching 3.5 μm. It should be noted that, compared to the N36 alloy, the microstructures in the longitudinal sections of the deformed samples of the 1N31 alloy are more distinct (Figs. 7d, 7f), and are characterized by considerably smaller minimum sizes of their elements. No reflections of the carbide phase were revealed in the electron diffraction patterns obtained when studying the 1N31 alloy, which indicates that the precipitates along the boundaries of the structure elements most likely represent amorphized carbon. Most elements of the structure of the transverse section have almost no elongation. The azimuthal misorientation of fragments inside the structure elements lies in the range of 2.5°–12°. Their size and the arrangement of the boundaries largely depend on the orientation of initial grains relative to the deformation direction. The dislocation density in the longitudinal and transverse sections is no more than $\rho = 10^{12}$ cm^{-2} and their distribution is more uniform than in the N36 alloy. Its increase in the deformed states of the 1N31 alloy compared to the N36 alloy is apparently associated with the fact that the dislocations are blocked by carbon atoms upon deformation due to the dissociation of graphite, which can promote a decrease in their mobility and, correspondingly, impede the formation of the cell structure.

The results of measurements of the Vickers hardness of alloys N36 and 1N31 in the initial state, as well as after upsetting to various degrees of deformation along the vertical axis of the samples are presented in Fig. 8. The hardness of the alloys N36 and 1N31 in the initial state is 160 and 253 HV_5, respectively. The analysis of the data obtained after the deformation of both alloys points to the nonuniformity of changes in the hardness over the section of the samples. The hardness gradually increases in the direction to the middle part of the sample $\left(\frac{h}{2}\right)$, which correlates with the larger degree of refinment of the structure in the center of the sample as compared to the periphery (Figs. 2c, 2d, 2g, 2h; Figs. 3c, 3d, 3g, 3h).

It should be noted that the hardness of the 1N31 samples in the initial state and after upsetting is higher in the near-surface layers by 100 HV_5 than in the N36 alloy, notably, 273–290 HV_5 and 185–190 HV_5, respectively, which is explained by an increase in the degree of the solid-solution and deformation-induced hardening associated with the carbon doping and effect of defect blocking. The latter is confirmed, not only by the higher hardness of the sample made of the 1N31 alloy, but also by an increased dislocation density to $\rho = 10^{12}$ cm^{-2} after upsetting compared to the N36 alloy ($\rho = 10^{11}$ cm^{-2}). Even more considerable post-deformation strengthening is observed in the central part of the billet made of the 1N31 alloy, which is indicated by a 23% increase in hardness (Fig. 8b), compared to a 15% increase for the N36 alloy (Fig. 8a). This distinction is caused by the fact that, in spite of the different changes in the coefficients of grain shape k_1 and k_1', for the 1N31 and N36 alloys (a decrease in the average grain size in the plane of measurements of the microhardness parallel to the upsetting direction, Table 2), the more effective refinment of the structure is observed in the center of the billet of the carbon-containing alloy, which is associated with carbon and the features of its distribution over the defects and boundaries of the structure elements (Figs. 2c, 2d, 2g, 2h; Figs. 3c, 3d, 3g, 3h; Fig. 8).

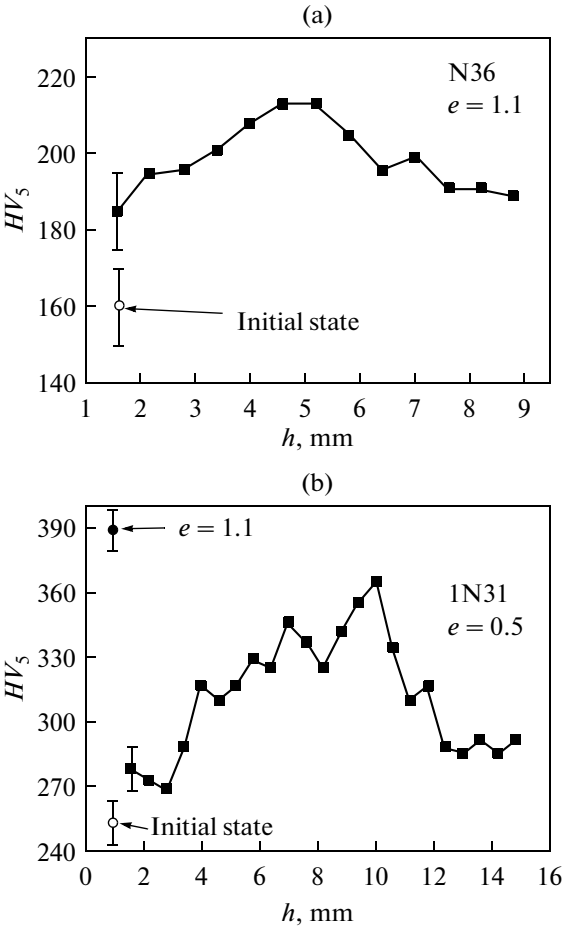

Fig. 8. Distribution of hardness (HV_5) over the sample height (h) of the alloys (a) N36 and (b) 1N31 after upsetting.

Thus, the general character of changes in the hardness of both alloys along the upsetting axis agrees with its behavior for other materials ([10], including the case with the imposition of ultrasonic vibrations [8]), which demonstrates a considerable excess in the carbon-containing alloy.

CONCLUSIONS

(1) The influence of the plastic deformation by upsetting to $e = 0.5$ and 1.1 on the changes in the dimensional and microstructural characteristics of the samples of invar fcc alloys Fe–35.0% Ni–0.49% Mn

and Fe–30.9% Ni–1.23% C has been investigated. The relationship between the coefficients of the relative changes in the billet sizes and grain forming in the alloys upon upsetting and their dependence on the composition has been found. The coefficient of elongation of the structure elements of the N36 deformed alloy decreases on moving from the contact surface in the direction to the sample middle; at the same time, in the 1N31 alloy, its decrease is minimized.

(2) Carbon in the initial state of the 1N31 alloy is distributed predominantly over grain boundaries. After upsetting of the carbon-containing alloy, in contrast to the N36 alloy, a clearer formation of boundaries is observed in the longitudinal sections, whereas the dislocation structure in the transverse sections of both alloys is constituted by tangled formations, with a higher defect density in the 1N31 alloy. The latter is accounted for by blocking of defects by carbon.

(3) A more substantial strengthening of the central part of billets of both alloys compared to the periphery after the upsetting deformation has been demonstrated (by 30 HV_5 at $e = 1.1$ for the N36 alloy and by 100 HV_5 at $e = 0.5$ for the 1N31 alloy), which is caused by the different forming of the structural elements in them. A considerable increase in hardness after upsetting in the carbon-containing alloy is associated not only with the more substantial refinement of all structural elements, but also with an increased density of dislocations blocked by carbon.

ACKNOWLEDGMENTS

This study was supported by the budget theme no. 022/10-B of the Institute of Metal Physics of the National Academy of Sciences of Ukraine.

REFERENCES

1. S. I. Gubkin, *Plastic Deformation of Metals*, Vols. 1–3 (Metallurgizdat, Moscow, 1960–1961) [In Russian].
2. J. Billigmann, *Stauchen und Pressen* (Carl Hansen-Verlag, München, 1953; MAShGIZ, Moscow, 1960).
3. P. G. Kirillov, *Theory of Metal Forming* (Vysshaya shkola, Moscow, 1965) [in Russian].
4. G. Ya. Gun, *Theoretical Foundations of Metal Forming* (Metallurgiya, Moscow, 1980) [in Russian].
5. S. A. Mashekov, G. G. Kurapov, U. K. Kakimov, and N. A. Bazhaev, "Upsetting of steel cylindrical samples," Vestn. Kazakh. Nat. Tech. Univ, No. 3, 79 (2010).
6. F. Blaha and B. Langenecker, "Plastizitätsuntersuchungen von Metallkristallen in Ultraschallfeld," Acta Metall. **7**, 93–100 (1959).
7. F. Blaha, B. Langenecker, and D. Oelschlägel, "Zum plastischen Verhalten von Metallen unter Schalleinwirkung," Z. Metallkd. **51**, 636–638 (1960).
8. O. Izumi, K. Oyama, and Yo. Suzuki, "Effects of super imposed ultrasonic vibration on compressive deformation of metals," Trans. JIM **7**, 162–167 (1966).
9. P. Yu. Volosevich, A. V. Kozlov, and B. N. Mordyuk, "Plastic deformation in ultrasonic field and its potential in the saturation of surface layers of iron samples by carbon," Metallofiz. Noveishie Tekhnol. **25**, 679–692 (2003).
10. V. Ya. Gerasimov and D. N. Paryshev, "Bauschinger effect upon upsetting of steel cylinders," Vestn. Mosk. Gos. Tekhn. Univ. im. G. I. Nosova, No. 1, 30–31 (2012).
11. V. G. Gavrilyuk and V. M. Nadutov, "Effect of carbon on the magnetic and atomic ordering in an Fe–Ni alloy," Fiz. Met. Metalloved. **56**, 555–563 (1983).

Translated by N. Korovin